DOI: 10.1002/chem.200501093

# Ultrafast Excited-State Excitation Dynamics in a Quasi-Two-Dimensional Light-Harvesting Antenna Based on Ruthenium(II) and Palladium(II) Chromophores

**Benjamin Dietzek,[a, d] Wolfgang Kiefer,[a] Jörg Blumhoff,[b] Lars Böttcher,[b] Sven Rau,[b] Dirk Walther,[b] Ute Uhlemann,[c] Michael Schmitt,[c] and Jürgen Popp*[c]**

**Abstract:** A detailed study on the excited-state-excitation migration taking place within the tetranuclear complex $[\{(tbbpy)_2Ru(tmbi)\}_2\{Pd(allyl)\}_2](PF_6)_2$ (tbbpy = 4,4′-di-*tert*-butyl-2,2′-bipyridine and tmbi = 5,6,5′,6′-tetramethyl-2,2′-bibenzimidazolate) is presented. The charge transfer is initiated by the photoexcitation into the lowest metal-to-ligand charge-transfer (MLCT) band of one of the peripheral ruthenium(II) chromophores and terminates on the central structurally complex $Pd_2^{II}(allyl)_2$ subunit. Thus, the system under investigation can be thought of as a functional model for the photosynthesis reaction center in plants. The kinetic steps involved in the overall process are inferred from femtosecond time-resolved transient-grating kinetics recorded at spectral positions within the regions of ground-state bleach and transient absorption. The kinetics features a complex non-exponential time behavior and can be fitted to a bi-exponential rise ($\tau_1 \geq 200$ fs, $\tau_2 \approx 1.5$ ps) and a mono- or bi-exponential decay, depending on the experimental situation. The data leads to the formulation of a model for the intramolecular excitation-hopping ascribing intersystem crossing and subsequent cooling as the two fastest observed processes. Following these initial steps, charge transfer from the ruthenium to the central complex $Pd_2(allyl)_2$ moiety is observed with a characteristic time constant of 50 ps. A 220-ps component that is observed in the ground-state recovery only is attributed to excitation equilibration between the two identical Pd(allyl) chromophores.

**Keywords:** artificial light-harvesting antenna · electron transfer · femtochemistry · heterometallic complexes · time-resolved spectroscopy

## Introduction

The substantial interest in the excited-state properties of transition-metal polypyridine complexes, in particular those that contain $d^6$ metals such as ruthenium, is largely motivated by their central role in addressing a wide variety of fundamental questions concerning the mechanisms of inter and intramolecular energy and electron transfer, charge localization, supramolecular chemistry, and inorganic light-harvesting.[1–9] Furthermore, interesting application possibilities arise from their potential use in photovoltaic devices such as dye-sensitized solar cells, optical data storage media, or in molecular devices.[10–13]

The generally accepted frame in which the excited-state properties of transition-metal polypyridine complexes are explained, exploits a very rapid light-induced population of the lowest-lying excited triplet state. The process of intersystem-crossing (ISC) from the originally excited singlet state

[a] Dr. B. Dietzek, Prof. Dr. W. Kiefer
Institut für Physikalische Chemie
Bayerische Julius-Maximilians Universität Würzburg
Am Hubland, 97074 Würzburg (Germany)

[b] Dipl.-Chem. J. Blumhoff, Dipl.-Chem. L. Böttcher, Dr. S. Rau, Prof. Dr. D. Walther
Institut für Anorganische Chemie
Friedrich-Schiller-Universität Jena
August-Bebel-Strasse 2, 07743 Jena (Germany)

[c] Dipl.-Chem. U. Uhlemann, Priv.-Doz. Dr. M. Schmitt, Prof. Dr. J. Popp
Institut für Physikalische Chemie
Friedrich-Schiller-Universität Jena
Helmholtzweg 4, 07743 Jena (Germany)
Fax: (+49) 3641-948-302
E-mail: juergen.popp@uni-jena.de

[d] Dr. B. Dietzek
Current address: Department of Chemical Physics
Lund University, P.O. Box 124, 22241 Lund (Sweden)

   

($^1$MLCT) to the lowest-lying metal-to-ligand charge-transfer triplet state ($^3$MLCT) can be extremely fast and was found to be in the order of 100 fs in $[Ru(bpy)_3]^{2+}$ (bpy = 2,2′-bipyridine).[14] Despite being a spin-forbidden process, ISC proceeds in this complex quite often with unitary efficiency and in conjunction with spin-allowed processes such as internal conversion (IC) and intramolecular vibrational energy redistribution (IVR).[14–17] The ultrafast intersystem-crossing is due to the pronounced heavy-atom effect caused by the central transition-metal ion, that induces strong spin–orbit coupling, and a relatively large number of unoccupied excited states that are available for excitation.[14,18,19] All subsequent photophysics following the ultrafast ISC is usually discussed starting from the $^3$MLCT state. However, important exceptions to the picture outlined above have been recently found; arguments have been put forward suggesting that the ISC might not proceed with unitary efficiency and is influenced by the surrounding solvent.[20] Schepp and co-workers present observations of a distinct three-state excited-state relaxation involving a singlet, a triplet, and furthermore, a state with mixed singlet–triplet character upon promoting the system into high-lying excited states by applying a wide range of excitation energies.[20d] The experiments presented in the following however are restricted to excitation of the complexes into the long-wavelength side of the MLCT absorption band. Therefore, we do not expect the higher-lying excited state manifold to influence our measurements.

Another important deviation from the generally accepted picture of the photophysics of ruthenium complexes was found by Sundstrøm and co-workers;[21] they report on light-induced processes in a multicenter Ru–Os complex, in which the ISC within the photoexcited ruthenium subunit competes with an extremely rapid (<60 fs) singlet–singlet Ru-to-Os energy transfer. Similar results were recently obtained by Campagna and co-workers.[22]

Despite these exceptions, it can be assumed that the photophysical behavior of supramolecular devices based on transition-metal polypyridine subunits originates in most cases from a rapidly populated $^3$MLCT state.[15–23] The issue of intramolecular charge and energy transfer from one subunit of the system to another is of particular interest in systems that are designed to serve as metal-based light-harvesting antennas.[24–28] Such systems containing more than one metal ion connected through covalently bound extended aromatic bridges can be basically described as independent centers between which charge transfer occurs.[29–30] This finding leads to the intuitive idea of the aromatic bridges as "molecular wires".[31,32]

Whereas most of current discussion focuses on the investigation of inter and intramolecular-electron and energy-transfer phenomena in ruthenium and osmium complexes[23,24,33,34] only limited data on heterooligonuclear complexes containing potentially reactive additional metal centers are available.[31,35,36] For a future implementation of photoredox processes it is in our view however extremely important to use auxiliary metal centers with extensively tunable redox properties to allow a much more widespread applicability of this concept. We will focus our investigation on a tetranuclear ruthenium–palladium complex [{bis[bis-(4,4′-di-*tert*-butyl-2,2′-bipyridine)ruthenium(II)-(5,6,5′,6′-tetramethyl-2,2′-bibenzimidazolate)]-bis{[1,3-allyl]palladium(II)}bishexafluorophosphate] ($Ru_2Pd_2$) and the mononuclear ruthenium complex [bis-(4,4′-di-*tert*-butyl-2,2′-bipyridine)ruthenium(II)-(5,6,5′,6′-tetramethyl-2,2′-bibenzimidazol)-bis-hexafluorophosphate] (Ru), which constitutes the chromphoric unit within the larger aggregate. The species under investigation, the mononuclear ($[(tbbpy)_2Ru(tmbiH_2)](PF_6)_2$) and the tetrametallic four-center complex ($[[\{(tbbpy)_2Ru(tmbi)\}_2\{Pd(allyl)\}_2](PF_6)_2$), hereafter referred to as the Ru complex and $Ru_2Pd_2$ complex respectively, are depicted schematically in Scheme 1 top and bottom.

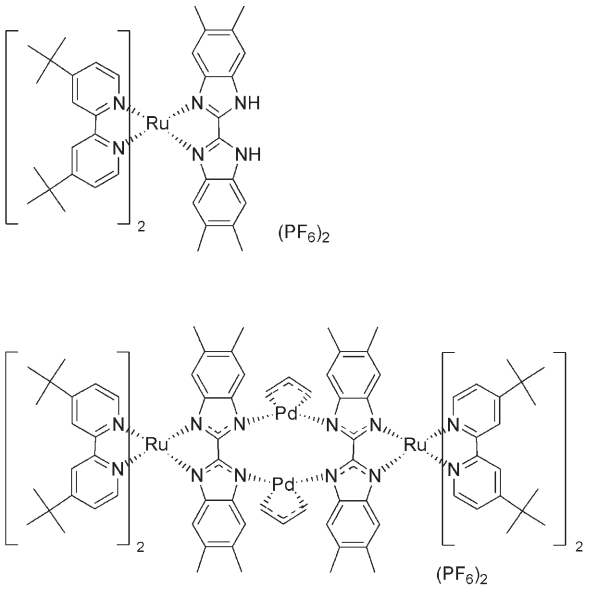


Scheme 1. The chemical structures of (top) $[(tbbpy)_2Ru(tmbiH_2)]$ and (bottom) $[\{(tbbpy)_2Ru(tmbi)\}_2[Pd(allyl)]_2](PF_6)_2$.

The discussion is organized as follows: After giving a brief overview over the experimental technique used in our experiments, we present and discuss the data obtained for the Ru complex that constitutes one of the chromophoric centers of the $Ru_2Pd_2$ complex. This complex is investigated in order to facilitate the interpretation of the data obtained for the $Ru_2Pd_2$ complex that is presented subsequently. To supplement the discussion, transient kinetics observed in the $[Ru(tbbpy)_3]^{2+}$ complex, which structurally differs from the $[(tbbpy)_2Ru(tmbiH_2)]^{2+}$ complex by the replacement of the bridging $tmbiH_2$ ligand with the tbbpy ligand, is added to the argument. To address the question of which particular ligand is involved in the process of photoexcitation, we refer to resonance Raman measurements that will be published in due course. The discussion of the photophysical properties of the $Ru_2Pd_2$ complex focuses on the interpretation of the multi-exponential decay processes that are related to the MLCT inherent charge-transfer events that move the excitation originally located on the Ru chromophore to the Pd

  

center. Thus, the complex can be viewed as a model for a small inorganic antenna system (the two ruthenium complexes) capable of transferring redox equivalents to a reaction center (the two palladium centers). However, in contrast to other inorganic light-harvesting systems the energy trap, the Pd subunit, is not surrounded in three dimensions by the light-harvesting Ru subunits but rather placed in the middle and therefore quite accessible for potential substrates (the X-ray data show that the complex is not flat but more like the roof of a house with the palladium unit representing the roof ridge). A detailed discussion of the structural features of $Ru_2Pd_2$ can be found in the literature.[37] Thus, we consider the $\{[(tbbpy)_2Ru(tmbi)]_2[Pd(allyl)]_2\}(PF_6)_2$ system to be an extremely interesting model of an inorganic antenna system with accessible reaction centers.

In the studies cited above, transient absorption spectroscopy, fluorescence up-conversion, and time-resolved fluorescence spectroscopy, as well as transient absorption anisotropy measurements have been exploited to gain a rich variety of information about the excited-state properties of transition-metal complexes and the light-induced processes in these substances. In the present study, to the best of our knowledge, we present the first femtosecond time-resolved four-wave-mixing study on the excited-state processes in Ru—bipyridine-based complexes. Transient-grating spectroscopy was chosen for this study as it is well established that this coherent technique yields excellent signal-to-noise ratios and thus allows for a very precise fitting of the transient data.[38–40] In order to facilitate the interpretation of the transient curves gained by the transient-grating method, we measured transient absorption data first. These data were taken with a poor time resolution and were solely used to obtain spectral information about the excited states of the investigated complexes.

## Experimental Section

**Materials**: The synthesis of the complexes and their structures are described elsewhere.[37,41,42] The complexes were dissolved in dichloromethane and acetone yielding an optical density of 1.5 in the 1-mm path-length cuvette, which was used for the time-resolved experiments. All solvents used in this study were HPLC grade as provided by the supplier (Aldrich).

**Femtosecond time-resolved spectroscopy**: The layout of the femtosecond laser system used in the experiments presented here has been described in detail elsewhere.[43] It basically consists of a Ti:sapphire oscillator and regenerative amplifier (CPA 1000, Clark MXR) producing pulses centered at 800 nm with a repetition rate of 1 kHz. The output of the system was split into two parts of equal power by means of a 1:1 beam splitter. For obtaining the transient absorption spectra one part of the fundamental 800 nm light was used to pump an optical parametric amplifier (OPA, TOPAS Light Conversion) to generate wavelength-tunable pump pulses. The pulses were chirp-compensated and recompressed by using a double-pass prism compressor yielding pulse durations of typically 100 fs. The second part of the amplifier output was used to generate a white-light continuum in a 3-mm sapphire window that served as the probe beam. A wedge was used to split of part of the white light forming the reference beam. The probe and the reference beam were sent to the detector consisting of a monochromator (SpectraPro 500, Acton) and a CCD camera (SDS 9000, Photometrics). The CCD chirp was split into two parts that could be read out independently. The chirp of the white light was compensated numerically during data processing.

For the transient grating (TG) experiments each part of the amplified 800 nm light was used to separately pump two optical parametric amplifiers (OPA, TOPAS Light Conversion) producing two independently tunable pulse trains that were chirp-compensated and recompressed independently. The pump pulses ($k_1$ and $k_2$) within the transient-grating scheme had the same color and were generated by dividing the output of one OPA into two beams of approximately the same intensity by means of a 1:1 beam splitter. The pulses produced by the second OPA served as the probe pulses ($k_3$) within the experimental scheme and were delayed with respect to the pump pulses by means of an optical delay line. In order to suppress any undesired anisotropy contributions to the TG signal the polarization of the probe beam was rotated by 54° with respect to the polarization of the pump beams, that is, the magic-angle configuration was employed.[44,45] All beams were made parallel and were focused onto the sample with a 20 mm spherical mirror. The pulse energies at the sample were typically 100 nJ, the sample itself was placed in rotating cell of 1-mm path length to avoid rapid photodegradation of the sample and thermal effects. The rotation speed was adjusted so that each set of pulses interacted with a fresh portion of the sample. Having passed the sample, the signal that was generated in the phase-matched direction ($k_{TG}=k_1-k_2+k_3$) was re-collected using a 50 mm focal-length achromatic lens and sent to the spectrometer detector unit to detect the transient grating signal spectrally dispersed as a function of the delay time between the pump and the probe pulse.

Absorption spectra of the sample were recorded before and after each measurement to monitor the integrity of the sample.

## Results and Discussion

**Ru complex**: The discussion of the excited-state properties of Ru will serve as a basis for the discussion of the photophysical processes occurring in the $Ru_2Pd_2$ complex, since the Ru complex constitutes the peripheral building blocks of the larger tetranuclear complex.

The absorption spectrum of the Ru complex dissolved in dichloromethane is shown in Figure 1 together with its luminescence and the luminescence excitation spectrum. The strong absorption band centered at 490 nm is due to the optically allowed transition that promotes a metal $d^6$ electron into a $^1$MLCT state located on an aromatic ligand. The luminescence occurs considerably red-shifted with respect to the excitation spectrum with a maximum at 650 nm and decays with a lifetime of 363 ns as determined from time-resolved luminescence measurements in THF.[37]

In our experiments we used 500-nm pump pulses to excite the complex within the $^1$MLCT band. Therefore, on the basis of the generally accepted description of the photophysics of Ru–polypyridine complexes we expect to observe a rapid formation of the long-lived $^3$MLCT state. The transient absorption spectrum taken 5 ps after photoexcitation into the $^1$MLCT band is shown in Figure 1B. Typical transient absorption features for this class of complexes are exhibited; a strong ground-state bleach (GSB) in the spectral region of the ground-state absorption is accompanied by a broad and featureless excited-state absorption at the red side of the ground-state bleach originating from excited singlet and triplet states. The slight red shift of the bleach max-

  

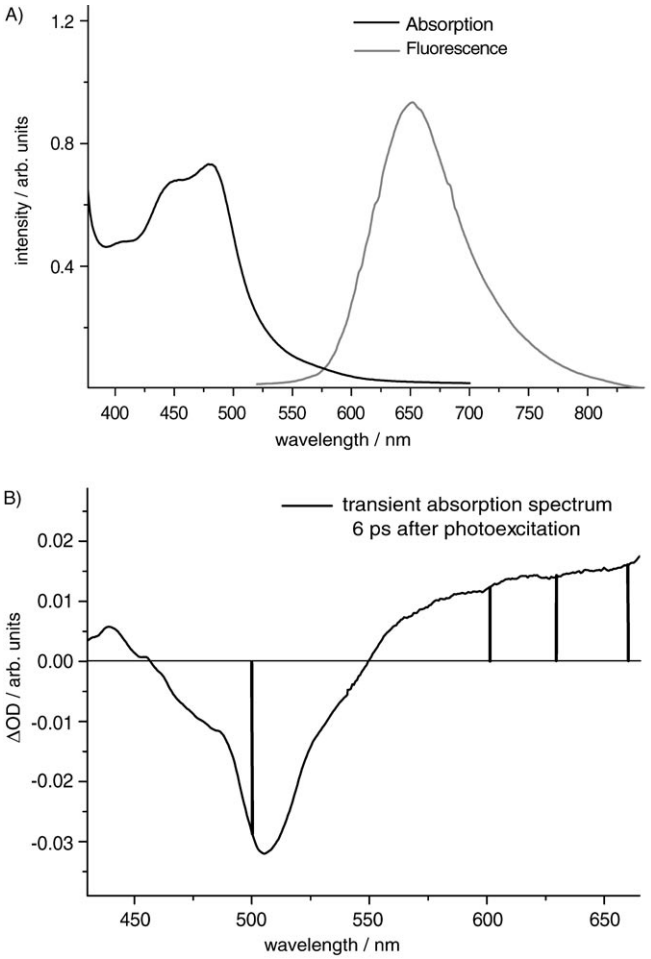


Figure 1. A) The steady-state absorption and the luminescence spectrum of $[(tbbpy)_2Ru(tmbiH_2)]$. The luminescence was excited at 460 nm. B) The transient absorption spectrum of $[(tbbpy)_2Ru(tmbiH_2)]$ taken 6 ps after photoexcitation into the MLCT band at 500 nm. The wavelengths used in the transient-grating measurements (pump at 500 nm and probe at 600, 630, and 660 nm) are indicated as vertical lines.

imum with respect to the maximum of the $^1$MLCT band is ascribed to minor contributions from stimulated emission.

The probe wavelengths applied for our TG measurements were chosen on the basis of the transient absorption spectrum and are indicated in Figure 1B. To probe the light-induced dynamics following photoexcitation at 500 nm, the probe laser was tuned to 600, 630, and 660 nm, thus monitoring the evolution of the broad photoinduced absorption band with time.

Figure 2A and B display transient-grating signals that were measured for a pump wavelength of 500 nm and probe wavelengths at 630 and 660 nm, respectively. The data presented in Figure 2 were acquired by using dichloromethane as solvent. All transients presented here exhibit a common feature: At zero delay time a signal is observed that peaks sharply and then rapidly decays. Following this spike the signals in Figure 2A and B rise within the first 5 ps and afterwards the TG signal is found to be constant.

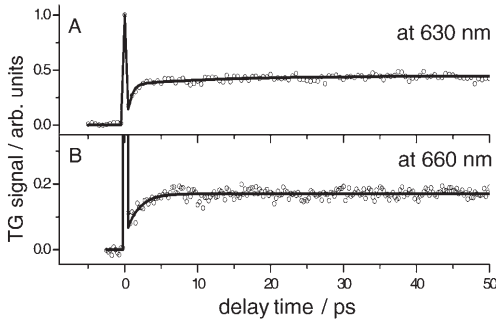


Figure 2. Transient-grating kinetics of $[(tbbpy)_2Ru(tmbiH_2)]$ dissolved in dichloromethane recorded in the spectral regions of transient absorption following excitation at 500 nm. The probe wavelengths are indicated in the individual panels. Data are shown as symbols while solid lines represent the results of least-square (LS) fits. The details concerning the fitting procedure and results are given in the text.

The peak at $t=0$ fs is a common feature in transient-grating spectroscopy and is called a "coherent artifact".[38–40] It results from a non-resonant scattering of the probe pulse from a grating that is formed by the two pump pulses. This scattering is independent of the presence of an optical resonance in the system under investigation and persists for delay times during which the three incoming laser pulses interact simultaneously with the sample.[46,47] Thus, the temporal profile of the coherent artifact is completely described by the convolution of the three laser pulses.[48] In contrast, the resonant contribution of the TG signal depends on whether the probe laser wavelength is tuned to a molecular resonance, that is, an excited-state or ground-state absorption. To exploit such molecular resonances for our TG experiments, the probe wavelengths were tuned to be resonant with the photoinduced absorption. In Figure 2 the resonant part of each of the TG signals displayed can be clearly observed for delay times larger than approximately 150 fs manifesting itself as an initial rise of the signal. After approximately 5 ps the signal stays constant over the range of delay times accessible in our measurements. To evaluate the data quantitatively, the transients were fitted to a bi-exponential rise and a Gaussian that was used to account for the non-resonant scattering contribution.[48–50] This procedure leads to a fast rise time $\tau_1$ of about 200 fs and a long time constant $\tau_2$ of about 2.5 ps. The process associated with the 200 fs time constant contributes to approximately 80% to the overall increase, while the 2.5 ps component is responsible for the remaining 20%. Table 1 summarizes the time constants $\tau_1$ and $\tau_2$ as well as the respective amplitudes $A_1$ and $A_2$ for various selected probe wavelengths lying within the transient absorption of the Ru complex. Considering these build-up time constants of the transient absorption, it can clearly be seen that the transient absorption spectrum taken 5 ps after the initial photoexcitation reflects the absorption properties of the lowest-excited-state of the complex.

To gain a more detailed insight into the processes populating this lowest $^3$MLCT state, TG measurements in ace-

  

Table 1. Summary of the parameters obtained from fitting the TG data of $[(tbbpy)_2Ru(tmbiH_2)]$ dissolved in dichloromethane and acetone. The typical absolute errors of both time constants and amplitudes range from 10 to 25%. The amplitudes $A_1$ and $A_2$ describing the relative contribution of the ultrafast (picosecond) rise component to the overall rise reflect the various excited-state absorption cross-sections of the states involved in the process.

| | $CH_2Cl_2$ | | | Acetone | |
|---|---|---|---|---|---|
| | at 600 nm | at 630 nm | at 660 nm | at 600 nm | at 630 nm |
| $\tau_1$[fs] | 180 | 325 | 200 | 190 | 195 |
| $A_1$ | 0.70 | 0.75 | 0.65 | 0.90 | 0.82 |
| $\tau_2$[ps] | 3.5 | 3.0 | 1.5 | 10.6 | 9.3 |
| $A_2$ | 0.30 | 0.25 | 0.35 | 0.10 | 0.18 |

tone, which is more polar than dichloromethane, were performed to test the influence of the polarity of the environment on the intramolecular charge transfer. Furthermore, if more than one excited triplet state would be involved in a process such as interligand charge transfer a change of the solvent polarity should significantly alter the observed kinetics. Figure 3 compares two TG transients of the Ru complex for a probe wavelength of 600 nm recorded in dichloromethane and acetone.

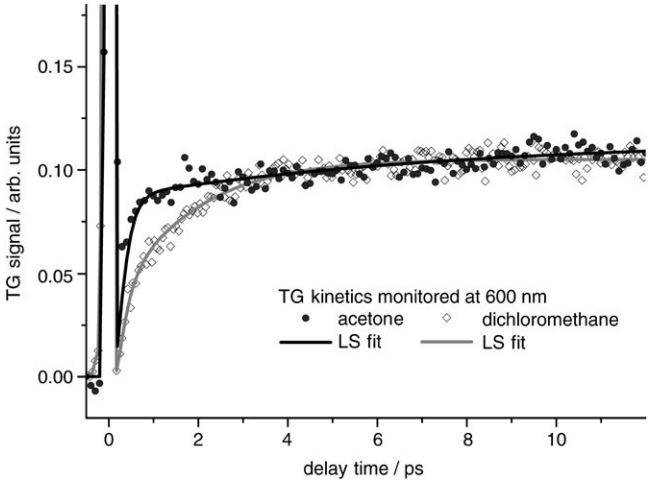


Figure 3. A comparison between the transient-grating kinetics measured at 600 nm of $[(tbbpy)_2Ru(tmbiH_2)]$ dissolved in acetone and in dichloromethane. Symbols represent data and results of LS fits are shown as solid lines.

It can be seen that the transients differ significantly. While the initial ultrafast rise times $\tau_1$ are very similar for both solvents the observed long time constant $\tau_2$ in acetone is roughly three times larger than the corresponding time constant observed for dichloromethane as solvent. On the basis of the results presented above and summarized in Table 1 we now discuss the processes that finally place the complex in its energetically most-favorable $^3$MLCT state.

The ultrafast rise time is attributed to the very rapid intersystem crossing (ISC) observed in Ru–bipyridine complexes that brings the system from an initially photoexcited $^1$MLCT state into the corresponding $^3$MLCT state. This ascription seems to be very likely considering the enormous amount of work published in the literature on similar molecular systems.[14,51]

We suggest that the observed long rise component can be attributed to cooling and solvent reorganization effects following the rapid $^1$MLCT$\rightarrow$$^3$MLCT ISC. This process has been reported in several articles dealing with similar Ru complexes[6,52,53] where it was found to take place in about 1 ps.[53] A red shift within the photoinduced absorption band typically associated with cooling is not observed as our experimental conditions only allowed us to measure transient absorption spectra up to 700 nm and therefore prevented us from recording the complete very broad photoinduced absorption spectrum extending far into the infrared. However, the observed solvent dependence is in excellent agreement with assigning the observed picosecond process to cooling. In contrast to the nearly plain energy dissipation observed in dichloromethane, the charge separation in the lowest-lying $^3$MLCT state triggers orientational changes in the more polar solvent acetone. This additional molecular motion causes the relaxation process to take place in about 10 ps and thus on a longer timescale than in the less polar solvent dichloromethane, in which mainly inner-shell reorganization has to be taken into account.

McFarland and co-workers reported on a picosecond component that they found when monitoring the picosecond luminescence of a homoleptic series of Ru complexes.[20] These authors present evidence for a distinct three-state excited-state relaxation behavior that can be observed when the systems used were excited with short wavelengths. Based on their very recent results, we would expect to observe a similar behavior in our complexes. Nonetheless, we are restricted to relatively low excitation photon energies and thus limited to excite our system into the red shoulder of the $d^6\rightarrow$$^1$MLCT transition. Therefore, we believe that in our experimental situation the model suggested by McCusker and co-workers[14,18] is valid and able to describe our data.

A yet different phenomenon, interligand charge transfer (ILCT), associated with time constants ranging from about 1 ps for structurally different types of ligands involved in the process of ILCT to about 100 ps for identical ligands but typically being in the order of 10 ps taking place in transition-metal complexes might also contribute to the observed bi-exponential rise.[54,55] To investigate the possibility of ILCT, we performed TG experiments on the $[Ru(tbbpy)_3]^{2+}$ complex, which structurally differs from the peripheral $Ru^{II}$ unit only by the replacement of the $tmbiH_2$ with a third tbbpy ligand. Figure 4 displays a comparison of a transient measured for each of the complexes. The data clearly shows the presence of a bi-exponential rise also for the $[Ru(tbbpy)_3]^{2+}$ complex. Furthermore, the observed ultrafast time constant of 150 fs and long rise time of 2.2 ps, are in excellent agreement with the time constants observed for $[Ru(tbbpy)_2(tmbiH_2)]$ (see Table 1). This finding indicates that identical processes contribute to the initial ultrafast rise of the TG signals in both $[Ru(tbbpy)_2(tmbiH_2)]$ and [Ru-

  

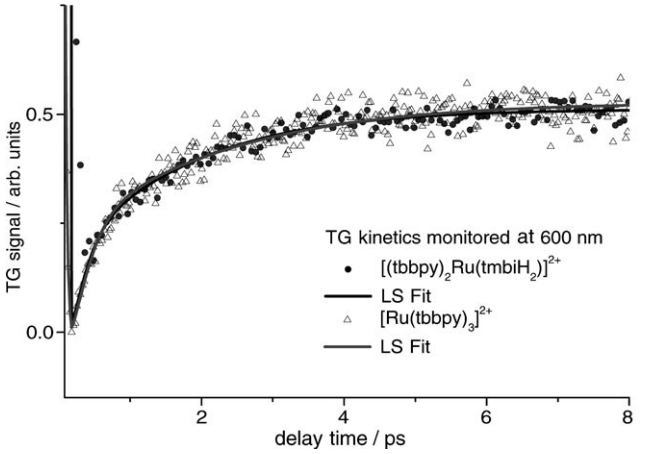


Figure 4. Transient-grating kinetics reflecting the time-evolution of the transient absorption are shown as measured for $[(tbbpy)_2Ru(tmbiH_2)]^{2+}$ and $[Ru(tbbpy)_3]^{2+}$ complexes dissolved in dichloromethane.

$(tbbpy)_3]^{2+}$ complexes. This conclusion is further substantiated by resonance Raman measurements showing that the modes coupled to the electronic $^1$MLCT transition are located on the tbbpy rather than on the bibenzimidazole ligand.[56] Thus, we conclude that ILCT between structurally different ligands cannot explain our experimental findings concerning the long rise time observed in the Ru complex.

In conclusion we interpret our data on the $[Ru(tbbpy)_2(tmbiH_2)]^{2+}$ complex as a rapid $\leq$200 fs $^1$MLCT$\rightarrow$$^3$MLCT ISC process followed by a cooling and solvent reorganization process within the $^3$MLCT state that takes place on a picosecond timescale. The interplay of both processes finally places the molecular system in its lowest excited state as schematically depicted in Figure 5. It is important to note that all relaxation dynamics within the excited-state manifold of the $Ru^{II}$ moiety are completed within about 10 ps. The resulting lowest-lying excited state was found to have a lifetime of 363 ns by performing nanosecond time-resolved luminescence experiments in THF.[37]

**RuPd complex**: Having discussed the ultrafast dynamic processes following initial photoexcitation of the $[(tbbpy)_2Ru(tmbiH_2)]$ complex, forming the peripheral building blocks of the four-center complex $[\{(tbbpy)_2Ru(tmbi)\}_2\{Pd(allyl)\}_2](PF_6)_2$, we will now focus on the latter system. The steady-state absorption and luminescence spectra of the $Ru_2Pd_2$ complex are shown in Figure 6A.

The strong absorption band at 530 nm is due to a $d^6\rightarrow$ $^1$MLCT transition within one of the ruthenium chromophores. The fact that this absorption feature is red-shifted compared with the absorption spectrum of the simple Ru complex as shown in Figure 1, reflects the interaction of the $Pd_2(allyl)_2$ moiety with the Ru centers.[57] The overall luminescence shows a maximum intensity at 658 nm and decays with a lifetime of 244 ns.[37]

Figure 6B displays the TA spectrum of the $Ru_2Pd_2$ complex taken 15 ps after photoexcitation of the system at 520 nm. The spectrum is dominated by a strong GSB in the region of the ground-state absorption. In the adjacent spectral regions photoinduced absorption bands can be observed; the one located on the blue side of the GSB is centered at 450 nm. As also found for the Ru complex, the second photoinduced absorption of the $Ru_2Pd_2$ complex manifests itself in a broad basically featureless band extending to the red of the ground-state bleach. For the TG experiments that were performed on the $Ru_2Pd_2$ complex dissolved in dichloromethane, we chose the probe wavelengths to be either resonant with the photoinduced absorption, that is, the probe laser was tuned to 600, 630, and 660 nm, or with the GSB, that is, the probe wavelength was set to be 480 or 520 nm, respectively.

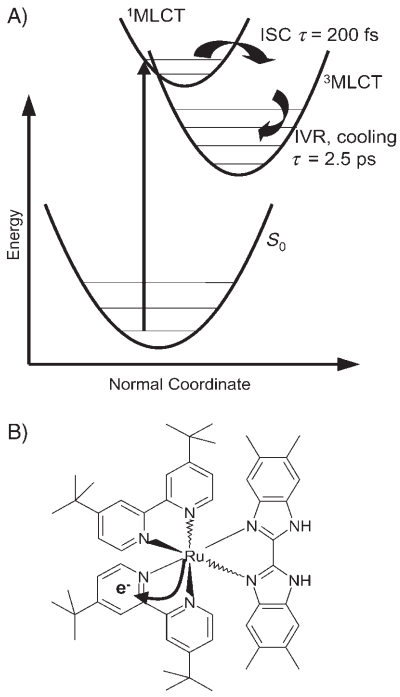


Figure 5. Schematic summarizing the ultrafast processes observed in $[(tbbpy)_2Ru(tmbiH_2)]$. A) A scheme involving the different states involved in the process; B) a localized picture of the charge excitation.

The transients excited at 520 nm and reflecting the time-dependence of the photoinduced absorption are shown in Figure 7. The data exhibit a coherent artifact as previously discussed for the Ru complex and a subsequent rise of the resonant part of the signal followed by a slower decay. For delay times larger than approximately 120 ps the signal intensity stays constant within the time range of 400 ps possible with our experimental setup. For a quantitative analysis of the data the resonant parts of the transients were fitted to a bi-exponential rise ($\tau_1$, $\tau_2$) multiplied with a sum of a mono-exponential decay ($\tau_3$) and a constant that was used to account for the long-lived constant signal.[49,50] Nanosecond time-resolved luminescence spectroscopy was used to characterize the lifetime of the long-lived state to be 244 ns.[37] A Gaussian centered at $t=0$ fs accounts for the coherent artifact.[48] This approach gives the time constants for the individual probe wavelengths that are summarized in

  

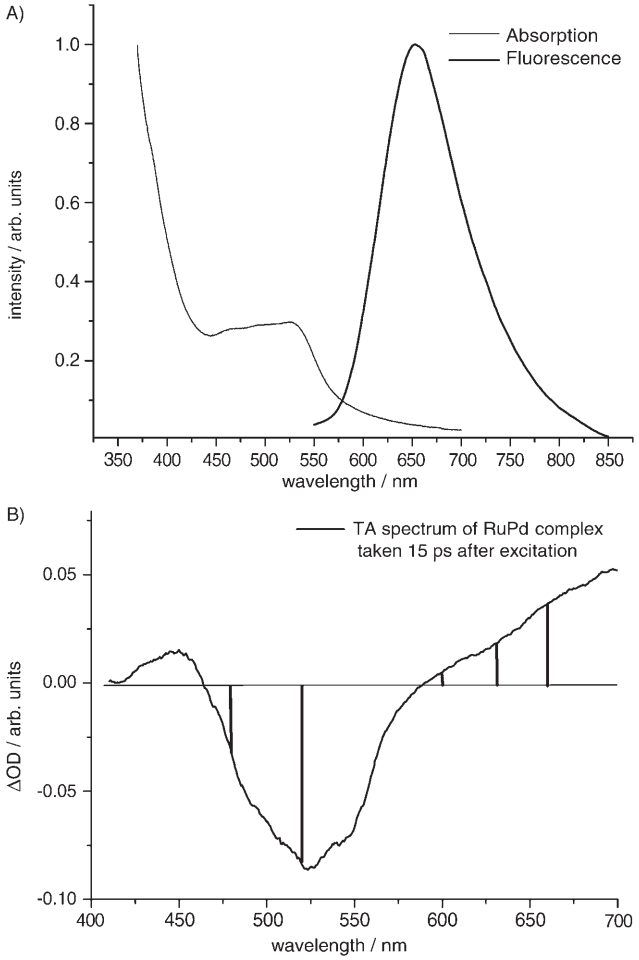


Figure 6. A) The steady-state absorption, luminescence, and luminescence-excitation spectra of $[\{(tbbpy)_2Ru(tmbi)\}_2\{Pd(allyl)\}_2](PF_6)_2$. The luminescence was excited at 520 nm and when recording the excitation spectrum the fluorescent intensity was monitored at 660 nm. B) The transient absorption spectrum of $[\{(tbbpy)_2Ru(tmbi)\}_2\{Pd(allyl)\}_2](PF_6)_2$ taken 20 ps after photoexcitation into the MLCT band at 500 nm. The wavelengths used to probe the transient-grating kinetics are indicated as vertical lines.

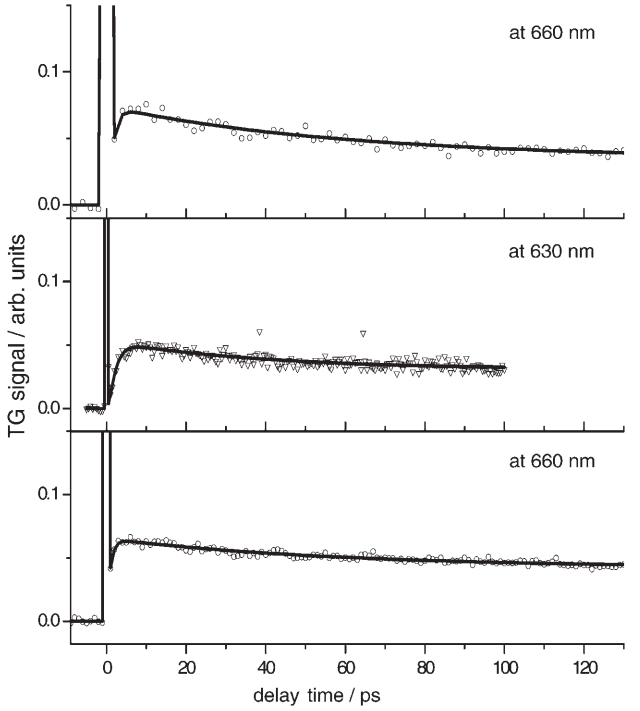


Figure 7. Transient-grating kinetics of $[\{(tbbpy)_2Ru(tmbi)\}_2\{Pd(allyl)\}_2](PF_6)_2$ dissolved in dichloromethane recorded in the spectral regions of transient absorption following excitation at 520 nm. The probe wavelengths are indicated in the individual panels. Data are shown as symbols while solid lines represent the results of LS fits. The details concerning the fitting procedure and results are given in the text.

Table 2. Summary of the parameters obtained from fitting the TG data of $[\{(tbbpy)_2Ru(tmbi)\}_2\{Pd(allyl)\}_2](PF_6)_2$ dissolved in dichloromethane. Time constants that appear as a rise of the TG signal at the given probe wavelengths are indicated with an asterisk. The amplitudes correspond to the relative contributions to the non-rising part of the signal. For comparison averaged values of the fitting parameters of $[(tbbpy)_2Ru(tmbiH_2)]$ are given in the last column. Typical errors of both time constants and amplitudes range from 10 to 25%.

| | RuPd | | | | | Ru |
|---|---|---|---|---|---|---|
| | at 480 nm | at 520 nm | at 600 nm | at 630 nm | at 660 nm | average |
| $\tau_1$ [fs] | 180 | 200 | $\leq 150$[a] | 180[a] | $\leq 150$[a] | 200[a] |
| $\tau_2$ [ps] | 1.2 | 0.8 | 1.3[a] | 1.7[a] | 1.1[a] | 2.1[a] |
| $\tau_3$ [ps] | 42.6 | 50.2 | 57.5 | 50.1 | 55.1 | – |
| $A_3$ | 0.17 | 0.26 | 0.30 | 0.32 | 0.20 | – |
| $\tau_4$ [ps] | 218 | 216 | – | – | – | – |
| $A_4$ | 0.73 | 0.65 | – | – | – | – |
| const | 0.10 | 0.09 | 0.70 | 0.78 | 0.80 | 1.00 |

[a] Data not taken in the region of predominant GSB.

Table 2; the values of the long rise-time constants $\tau_2$ range from 1.4 to 2.2 ps while the ultrafast rise component $\tau_1$ can be characterized by a time constant $\leq 180$ fs. To clearly demonstrate the bi-exponential nature of the initial rise, an enlarged view of the transient probed at 636 nm is presented in Figure 8A, while Figure 8B shows a direct comparison of TG data obtained for the Ru and the $Ru_2Pd_2$ complex.

The decay observed for all probe wavelengths within the spectral range of the photoinduced absorption can be described by a time constant $\tau_3 = 50$–$58$ ps. For the transients probed within the photoinduced absorption band the process described by $\tau_3$ contributes to approximately 27% to the overall non-rising signal, while we attribute the remaining 73% to the long-lived component that appears as a constant in our measurements.

Having discussed the experimental data measured within the spectral region of photoinduced absorption, we now focus on transients by monitoring the time-evolution of the GSB. Table 2 also contains the values of the fitting parameters obtained from fitting the TG signals for probe wavelengths being resonant with the overall GSB; the corresponding transients are plotted in Figure 9. We see that if the probe laser is tuned to interrogate the ground-state recovery dynamics, the approach of fitting a bi-exponential rise followed by a mono-exponential decay to the data fails. Instead, a multi-exponential decay subsequent to the coher-

  

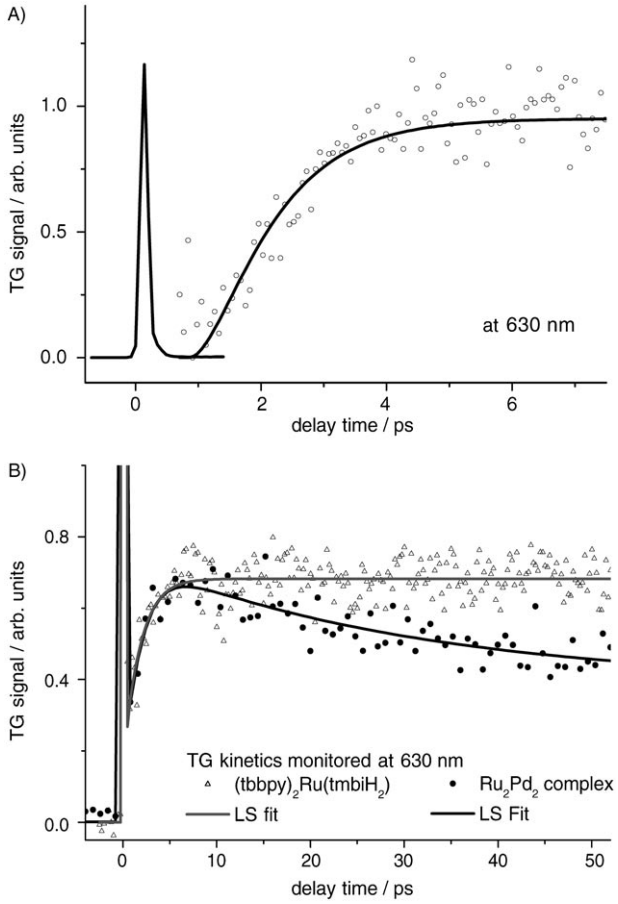


Figure 8. A) Transient-grating data of $[\{(tbbpy)_2Ru(tmbi)\}_2\{Pd(allyl)\}_2](PF_6)_2$ recorded at 630 nm. The expanded view on the ultrafast rise of the resonant part of the signal reveals the bi-exponential nature of this part of the signal. This part of the signal was enlarged with respect to the signal recorded around $t=0$ fs to better emphasize the rise characteristics of the signal. B) The direct comparison of the photoinduced absorption kinetics of the $Ru^{II}$ subunit and the tetranuclear complex. In both cases $CH_2Cl_2$ was used as solvent.

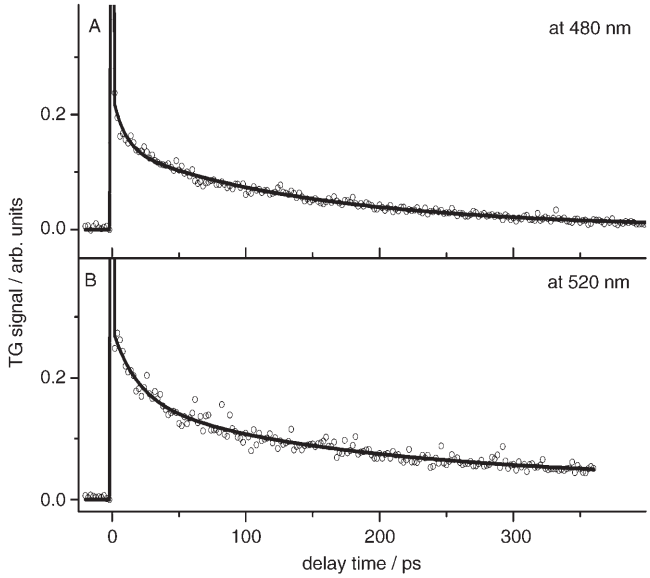


Figure 9. Transient-grating kinetics of $[\{(tbbpy)_2Ru(tmbi)\}_2\{Pd(allyl)\}_2](PF_6)_2$ dissolved in dichloromethane recorded in the spectral regions of ground-state bleach following excitation at 520 nm. The probe wavelengths are indicated in the individual panels. Data are shown as symbols while solid lines represent the results of LS fits. The details concerning the fitting procedure and results are given in the text.

ent artifact has to be employed to model the data shown in Figure 9. To obtain sufficiently satisfactory fits a long decay constant $\tau_4$ in the order of 220 ps has to be taken into account in addition to the time constants used to fit the data taken for probe wavelengths $\geq$600 nm resonant with the excited-state absorption. The additional slow process that is only present while monitoring the kinetics reflecting the time-dependence of ground-state recovery contributes to about 69%, the process associated with $\tau_3$ to 22%, and the process that appears as a constant within our time resolution to 9% to the overall signal.

We will now discuss the results of the TG measurements on the $Ru_2Pd_2$ complex summarized in Table 2 in more detail to obtain a complete picture of the photoinduced processes in the $Ru_2Pd_2$ complex. We will also include our considerations about the relaxation processes in the $[(tbbpy)_2Ru(tmbiH_2)]$ complex.

The strikingly similar values of the short time constants $\tau_1$ and $\tau_2$ obtained for the $[(tbbpy)_2Ru(tmbiH_2)]$ complex ($\tau_1 \leq$ 220 fs, $\tau_2 \approx 2.5$ ps), as well as for $Ru(tbbpy)_3$ used as a reference system, and the $Ru_2Pd_2$ complex ($\tau_1 \leq 200$ fs, $\tau_2 \approx 1.3$ ps) lead to the conclusion that these time constants are associated with the same overall processes in all systems. This assumption is further supported by the fact that multicenter transition-metal complexes can successfully be described based on the assumption of two (or more) independent chromophores that are only weakly coupled.[29–32] Furthermore, the initial excitation occurs on one of the peripheral Ru chromophores. Hence, in accordance with our previously discussed results, we ascribe all dynamics observed for delay times $\leq$10 ps to relaxation processes within the peripheral Ru subunits. Thus, we ascribe $\tau_1$ and $\tau_2$ to a rapid ISC, promoting the system from a $^1$MLCT to the $^3$MLCT state located on the Ru chromophore, and subsequent cooling and IVR within this state, respectively. Hence, the processes associated with $\tau_1$ and $\tau_2$ lead to the build-up of the photoinduced absorption of the Ru-$^3$MLCT state.

When investigating the photoinduced dynamics of the Ru complex dissolved in $CH_2Cl_2$ no kinetic component with a characteristic time constant larger than 3.5 ps has been observed. Therefore, we conclude that the existence of the slower components ($\tau_3 \approx 50$ ps and $\tau_4 \approx 220$ ps), which can be only seen for $Ru_2Pd_2$ is due to the complex structure of the tetranuclear antenna and the interaction of the peripheral Ru units and the complex central $Pd_2(allyl)_2$ moiety. As the processes associated with $\tau_3$ and $\tau_4$ originate from the presence of multiple chromophores within the complex, we assign the corresponding relaxation processes to charge transfer and subsequent equilibration. In particular, we as-

  

cribe the process manifesting itself as a $\approx$50 ps decay in the photoinduced absorption to an excitation transfer from a Ru–$^3$MLCT state to the one of the central Pd(allyl) moieties. This Ru–$^3$MLCT$\rightarrow$Pd(allyl) excitation-hopping reflects itself also in the spectral region of the overall GSB. The values of $\tau_3$ obtained from fitting the data within the excited-state absorption band correlate well with those used for fitting the transients monitoring the ground-state recovery kinetics.

We now discuss the slow decay that takes place on a 220-ps timescale and is solely observed when monitoring the ground-state recovery. Recalling the lifetime of the $Ru_2Pd_2$ complex to be 244 ns might lead to the speculation that the 220 ps time constant corresponds to a non-fluorescent transition back to the ground state that is too fast to be monitored within the time-resolution of the nanosecond experiment. Nevertheless, such a process should be visible both in the photoinduced absorption as well as in the GSB of the complex. Since the transients probing in the excited-state absorption do not exhibit a 220 ps component, we discard this model. For the same reasons back-electron-transfer from the $Pd_2(ally)_2$ unit to the ruthenium moieties is excluded to account for the slow kinetic component. As Ru$\rightarrow Pd_2(allyl)_2$ electron transfer is indicated, when monitoring the time-dependence of the photoinduced absorption band, the reverse process should be observed in a corresponding manner. However, the 220-ps process is solely observed when monitoring the ground-state recovery and cannot be seen when monitoring the transient absorption of the sample. Thus, neither a non-radiative transition back into the ground state nor back-electron-transfer account for our experimental findings of a 220-ps component. Instead we suggest that the slow dynamic component is due to an excitation transfer between the two chemically identical Pd(allyl) centers, thus leading to a situation in which the excitation is equally distributed over both Pd(allyl) centers. Within this scenario one would expect to observe no spectral changes in the excited-state absorption of the system, as corresponding states of either Pd(allyl) center exhibit identical absorption properties. However, the process of intercenter excitation transfer (ICET) (see Figure 10) manifests itself in the GSB kinetics as it leads to a fully equilibrated excited state and thus precedes complete ground-state recovery. This model of ICET following excitation transfer from the ruthenium subunits to the central $Pd_2(allyl)_2$ moiety is consistent with the relative contributions of the components visible in our data as summarized in Table 2. Within the GSB the process associated with $\tau_4$ and the constant approximately corresponds to the constant within the photoinduced absorption band, while the contributions of $\tau_3$ are about the same in both spectral regions; for example, $A_4$ and the constant resulting from a fit of the data taken at 520 nm sum up to 0.74 that is consistent with the average value of 0.76 of the constant obtained from fitting the transients taken in the spectral region of photoinduced absorption (for details see Table 2). This finding implies the presence of a sequential process rather than concurrent relaxation pathways, with the slow contribution being unobservable when monitoring the kinetics of the excited-state absorption band.

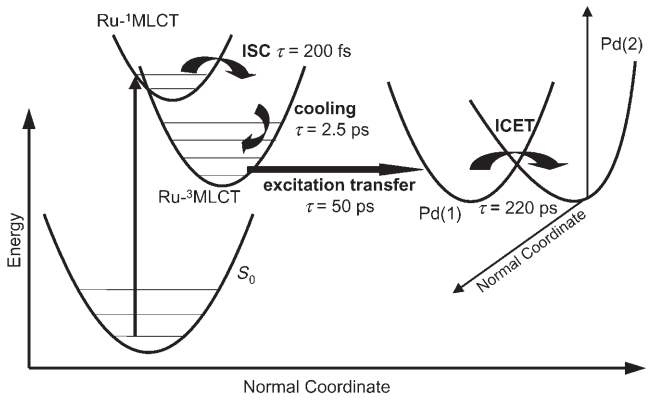


Figure 10. The kinetic processes observed in the $[\{(tbbpy)_2Ru(tmbi)\}_2\{Pd(allyl)\}_2](PF_6)_2$ are depicted schematically. Left: A scheme involving the different states involved in the excited-state relaxation processes initiated by photoexcitation at 520 nm. Right: A local picture of the charge transfer.

In contrast to ILCT taking place between two distinguished ligands within the same chromophoric center, the ICET, as apparent in the data presented here, takes place between two identical chromophoric centers that have the same energy positions of their excited states. Thus a strong driving force for an ICET due to the existence of an energetically favorable state located on one of the chromophoric centers is absent.[30] Therefore, the observed relatively long time-constant that we ascribe to the process of ICET becomes reasonable. Figure 10 schematically summarizes the kinetic processes observed in the $Ru_2Pd_2$ complex.

## Conclusion

Herein we have presented a detailed kinetic study of the excitation migration processes in the tetranuclear transition-metal complex $[\{(tbbpy)_2Ru(tmbi)\}_2\{Pd(allyl)\}_2](PF_6)_2$, which may serve as a model system for a small inorganic light-harvesting antenna or as a simple model for a photosynthesis reaction center. To facilitate the interpretation of the complex kinetic data, the peripheral building block of $[(tbbpy)_2Ru(tmbiH_2)]$ was included in our studies. We monitored the ultrafast excited-state relaxation processes leading to the equilibrated lowest-lying excited state of the complexes by means of femtosecond time-resolved transient-grating spectroscopy. By recording the TG kinetics in the spectral regions of ground-state bleach and transient absorption in combination with solvent-dependent measurements, we were able to assign a distinct kinetic process to each of the observed time constants. In isolated $[(tbbpy)_2Ru(tmbiH_2)]$ a rapid $\leq$200-fs $^1$MLCT$\rightarrow^3$MLCT ISC is followed by cooling and solvent reorganization leading to a fully thermalized $^3$MLCT excited state on a picosecond timescale. Time-resolved luminescence spectroscopy with nanosecond time-resolution reveals that this lowest-lying excited state in the

  

ruthenium complex decays with a characteristic time constant of 260 ns.

In $[\{(tbbpy)_2Ru(tmbi)\}_2\{Pd(allyl)\}_2](PF_6)_2$ additional time constants are observed; the one being in the order of 50 ps is attributed to a charge transfer from an excitation centered at a ruthenium chromophore to one of the Pd(allyl) moieties located in the central part of the tetranuclear complex. The slowest process apparent in the data is characterized by a time constant of 220 ps. As it is observed only in the ground-state recovery kinetics but not in the excited-state absorption, we conclude that this component is due to an intercenter excitation-hopping process. This process finally leads to an excitation that is equally distributed between both Pd(allyl) centers of the four-center transition-metal complex. The lifetime of this lowest-lying state was found to be 244 ns.

Finally, from a technical point of view, we believe that femtosecond time-resolved transient-grating spectroscopy is a powerful tool to elucidate relaxation processes even in complex systems and to address questions concerning the ultrafast photophysical mechanisms in charge-transfer systems.

## Acknowledgements

This work was financially supported by the Deutsche Forschungsgemeinschaft, through the grant Sonderforschungsbereich 436 (Metallvermittelte Reaktionen nach dem Vorbild der Natur, TP C1, A1, and A10). Benjamin Dietzek gratefully acknowledges financial support from the Studienfonds der Chemischen Industrie Deutschlands. Financial support from the Fonds der Chemischen Industrie is also highly acknowledged.

[1] J. M. Lehn, *Supramolecular Chemistry*, Wiley-VCH, Weinheim, **1995**.
[2] V. Balzani, A. Credi, M. Venturi, *Molecular Devices and Machines*, Wiley-VCH, Weinheim, **2003**.
[3] C. N. Fleming, K. A. Maxwell, J. M. DeSimone, T. J. Meyer, J. M. Papanikolas, *J. Am. Chem. Soc.* **2001**, *123*, 10336–10347.
[4] A. Vlcek, J. Heyrovsky, *Electron Transfer in Chemistry, Vol. 2* (Ed.: V. Balzani), Wiley-VCH, Weinheim, **2001**, and references therein.
[5] F. Scandola, C. Chiorboli, M. T. Indelli, M. A. Rampi, *Electron Transfer in Chemistry, Vol. 3* (Ed.: V. Balzani), Wiley-VCH, Weinheim, **2001**, and references therein.
[6] H. Torieda, K. Nozaki, A. Yoshimura, T. Ohno, *J. Phys. Chem. A* **2004**, *108*, 4819–4829.
[7] S. Welter, K. Brunner, J. W. Hofstraat, L. De Cola, *Nature* **2003**, *421*, 54–57.
[8] O. Bossart, L. De Cola, S. Welter, G. Calzaferri, *Chem. Eur. J.* **2004**, *10*, 5771–5775.
[9] A. Sautter, B. Kükrer Kaletas, D. G. Schmid, R. Dobrawa, M. Zmine, G. Jung, I. H. M. van Stokkum, L. De Cola, R. M. Williams, F. Würthner, *J. Am. Chem. Soc.* **2005**, *127*, 6719–6729.
[10] B. O'Regan, M. Grätzel, *Nature* **1991**, *353*, 737–739.
[11] G. Benkö, J. Kallioinen, J. E. I. Korppi-Tommola, A. P. Yartsev, V. Sundstrøm, *J. Am. Chem. Soc.* **2002**, *124*, 489–493.
[12] a) G. Calzaferri, S. Huber, H. Maas, C. Minkowski, *Angew. Chem.* **2003**, *115*, 3860–3888; *Angew. Chem. Int. Ed.* **2003**, *42*, 3732–3758.
[13] P. R. Hania, R. Telesca, L. N. Lucas, A. Pugyls, J. van Esch, B. L. Feringa, J. G. Snijders, K. Duppen, *J. Phys. Chem. A* **2002**, *106*, 8498–8507.
[14] N. H. Damrauer, G. Cerullo, A. Yeh, T. R. Boussie, C. V. Shank, J. K. McCusker, *Science* **1997**, *275*, 54–57.
[15] A. Juris, V. Balzani, F. Barigeletti, S. Campagna, P. Belser, A. von Zelewsky, *Coord. Chem. Rev.* **1988**, *84*, 85–277.
[16] P. C. Bradley, N. Kress, B. A. Hornberger, R. F. Dallinger, W. H. Woodruff, *J. Am. Chem. Soc.* **1981**, *103*, 7441–7446.
[17] L. F. Cooley, P. Bergquist, D. F. Kelley, *J. Am. Chem. Soc.* **1990**, *112*, 2612–2617.
[18] J. Monat, J. K. McCusker, *J. Am. Chem. Soc.* **2000**, *122*, 4092–4097.
[19] J. Kallioninen, G. Benkö, V. Sundstrøm, J. E. I. Korppi-Tommola, A. Yartsev, *J. Phys. Chem. B* **2002**, *106*, 4396–4404.
[20] a) W. R. Browne, G. C. Coates, C. Brady, P. Matousek, M. Towrie, S. W. Botchway, A. W. Parker, J. G. Vos, J. J. McGarvey, *J. Am. Chem. Soc.* **2003**, *125*, 1706–1707; b) W. R. Browne, G. C. Coates, C. Brady, P. Matousek, M. Towrie, S. W. Botchway, A. W. Parker, J. G. Vos, J. J. McGarvey, *J. Am. Chem. Soc.* **2004**, *126*, 10190–10190; c) G. B. Shaw, D. J. Styers-Barnett, E. Z. Gannon, J. C. Granger, J. M. Papanikolas, *J. Phys. Chem. A* **2004**, *108*, 4998–5006; d) S. A. McFarland, F. S. Lee, K. A. W. Y. Cheng, F. L. Cozens, N. P. Schepp, *J. Am. Chem. Soc.* **2005**, *127*, 7065–7070, and references therein.
[21] J. Andersson, F. Puntoriero, S. Serroni, A. Yartsev, T. Polivka, S. Campagna, V. Sundstrøm, *Chem. Phys. Lett.* **2004**, *386*, 336–341.
[22] F. Puntoriero, S. Serroni, M. Galletta, A. Juris, A. Licciardello, C. Chiorboli, S. Campagna, F. Scandola, *ChemPhysChem* **2005**, *6*, 129–138.
[23] V. Balzani, A. Juris, M. Venturi, S. Campagna, S. Serroni, *Chem. Rev.* **1996**, *96*, 759–833.
[24] S. Campagna, S. Serroni, F. Puntoriero, C. Di Pietro, V. Ricevuto, *Electron Transfer in Chemistry, vol. 5* (Ed.: V. Balzani), Wiley-VCH, Weinheim, **2001**, pp. 186–214, and references therein.
[25] C. A. Bignozzi, J. R. Schoonover, F. Scandola, *Prog. Inorg. Chem.* **1997**, *44*, 1–95.
[26] F. Barigeletti, L. Flamigni, *Chem. Soc. Rev.* **2000**, *29*, 1–12.
[27] T. J. Meyer, *Acc. Chem. Res.* **1989**, *22*, 163–170.
[28] J. S. Hsiao, B. P. Krueger, R. W. Wagner, T. E. Johnson, J. K. Delaney, D. C. Mauzerall, G. R. Fleming, J. S. Lindsey, D. F. Bocian, R. J. Donohoe, *J. Am. Chem. Soc.* **1996**, *118*, 11181–11193.
[29] V. A. Durante, P. C. Ford, *J. Am. Chem. Soc.* **1975**, *97*, 6898–6900.
[30] L. Flamigni, S. Encinas, F. Barigeletti, F. M. MacDonnell, K. J. Kim, F. Puntoriero, S. Campagna, *Chem. Commun.* **2000**, 1185–1186.
[31] M. L. A. Abrahamsson, H. B. Baudin, A. Tran, C. Philouze, K. E. Berg, M. K. Raymond-Johannson, L. Sun, B. Åkermark, S. Styring, L. Hammarstrom, *Inorg. Chem.* **2002**, *41*, 1534–1544.
[32] C. Chiorboli, M. A. J. Rodgers, F. Scandola, *J. Am. Chem. Soc.* **2003**, *125*, 486–491.
[33] R. T. F. Jukes, V. Adamo, F. Hartl, P. Belser, L. De Cola, *Coord. Chem. Rev.* **2005**, *249*, 1327–1335.
[34] L. De Cola, P. Belser, *Coord. Chem. Rev.* **1998**, *177*, 301–346.
[35] a) S. Ott, M. Kritikos, B. Åkermark, L. Sun, R. Lomoth, *Angew. Chem. Int. Ed.* **2004**, *43*, 1006–1009; b) S. Ott, M. Kritikos, B. Åkermark, L. Sun, R. Lomoth, *Angew. Chem.* **2004**, *116*, 1024–1027.
[36] J. D. Lee, L. M. Vrana, E. R. Bullock, K. J. Brewer, *Inorg. Chem.* **1998**, *37*, 3575–3580.
[37] D. Walther, L. Böttcher, J. Blumhoff, S. Schebesta, H. Görls, K. Schmuck, S. Rau, M. Rudolph, *Eur. J. Inorg. Chem,* in press.
[38] B. Dietzek, R. Maksimenka, G. Hermann, W. Kiefer, J. Popp, M. Schmitt, *ChemPhysChem* **2004**, *5*, 1171–1177.
[39] T. Siebert, V. Engel, A. Materny, W. Kiefer, M. Schmitt, *J. Phys. Chem. A* **2003**, *107*, 8355–8362.
[40] B. Dietzek, R. Maksimenka, W. Kiefer, G. Hermann, J. Popp, M. Schmitt, *Chem. Phys. Lett.* **2005**, *415*, 94–99.
[41] S. Rau, L. Böttcher, S. Schebesta, M. Stollenz, H. Goerls, D. Walther, *Eur. J. Inorg. Chem.* **2002**, *11*, 2800–2809.
[42] S. Rau, B. Schaefer, A. Gruessing, S. Schebesta, K. Lamm, J. Vieth, H. Goerls, D. Walther, M. Rudolph, U. W. Grummt, E. Birkner, *Inorg. Chim. Acta* **2004**, *357*, 4496–4503.
[43] M. Schmitt, G. Knopp, A. Materny, W. Kiefer, *J. Phys. Chem. A* **1998**, *102*, 4059–4065.
[44] L. D. Book, A. E. Ostafin, N. Ponomarenko, J. R. Norris, N. F. Scherer, *J. Phys. Chem. B* **2000**, *104*, 8295–9307.

  

[45] H. Maekawa, K. Ohta, K. Tominaga, *J. Phys. Chem. A* **2004**, *108*, 9484–9491.
[46] N. Kohles, P. Aechter, A. Laubereau, *Opt. Commun.* **1988**, *65*, 391–396.
[47] H. A. Ferwerda, J. Terspsta, D. A. Wiersma, *J. Chem. Phys.* **1989**, *91*, 3296–3305.
[48] J. Stenger, D. Madsen, J. Dreyer, P. Hamm, E. T. J. Nibbering, T. Elsaesser, *Chem. Phys. Lett.* **2002**, *354*, 256–263.
[49] D. M. Mittleman, R. W. Schoenlein, J. J. Shiang, V. L. Colvin, A. P. Alivisatos, C. V. Shank, *Phys. Rev. B* **1994**, *49*, 14435–14447.
[50] Y. Nagasawa, S. A. Passino, T. Joo, G. R. Fleming, *J. Chem. Phys.* **1997**, *106*, 4840–4852.
[51] J. N. Demas, G. A. Crosby, *J. Am. Chem. Soc.* **1971**, *93*, 2841–2847.
[52] A. T. Yeh, C. V. Shank, J. K. McCusker, *Science* **2000**, *289*, 935–938, and N. H. Damrauer, J. K. McCusker, *J. Phys. Chem. A* **1999**, *103*, 8440–8446.
[53] A. C. Bhasikuttan, M. Suzuki, A. Nakashima, T. Okada, *J. Am. Chem. Soc.* **2002**, *124*, 8398–8405.
[54] G. Benkö, J. Kallioinen, P. Myllyperkio, F. Trif, J. E. I. Korppi-Tommola, A. Yartsev, V. Sundström, *J. Phys. Chem. B* **2004**, *108*, 2862–2867, and references therein.
[55] G. B. Shaw, C. L. Grown, P. M. Papanikolas, *J. Phys. Chem. A* **2002**, *106*, 1483–1495.
[56] C. Herrmann, U. Uhlemann, B. Dietzek, S. Rau, M. Schmitt, J. Popp, M. Reiher, unpublished results.
[57] S. Rau, T. Büttner, C. Temme, M. Ruben, H. Görls, D. Walther, M. Duati, S. Fanni, J. G. Vos, *Inorg. Chem.* **2000**, *39*, 1621–1624.

Received: September 5, 2005
Revised: January 26, 2006
Published online: April 21, 2006

  